Probing Interactions of γ-Alumina with Water via Multinuclear Solid-State NMR Spectroscopy

Li Shen+,[a, b] Yang Wang+,[a] Jia-Huan Du,[a] Kuizhi Chen,[c] Zhiye Lin,[a] Yujie Wen,[a] Ivan Hung,[c] Zhehong Gan,[c] and Luming Peng*[a]

Interactions of γ-alumina with water are important in controlling its structure and catalytic properties. We apply solid-state multinuclear NMR spectroscopy to investigate these interactions by monitoring ^1H and ^{17}O spectra in real-time. Surface-selective detection is made possible by adsorbing ^{17}O-enriched water on γ-alumina nanorods. Structural evolution on the surface was selectively probed by ^1H/^{17}O double resonance NMR and ^{27}Al NMR at ultrahigh 35.2 T magnetic field. Formation of hydroxyl species on the surface of nanorods is rapid upon the exposure of water, which involves low coordinated aluminum ions with doubly bridging and isolated hydroxyl species being generated first. Fast exchange occurs between oxygen atoms in the water molecules and bare surface sites, indicating high reactivity of these oxygen species. These results provide new insights into the structure and dynamics on the surface of γ-alumina and the methods applied here can be extended to study the interaction of other oxides with water.

Due to its low cost,[1] high surface activity and large surface area,[2] γ-alumina has become one of the most important catalytic materials, both as the industrial catalysts and catalytic supports.[3] Since the surface structure of γ-alumina determines its catalytic properties, detailed structural information is required in order to further improve the performances of the catalyst. In particular, the nature and concentrations of hydroxyl sites on the surface play a crucial role.[4] Therefore, the surface structure of γ-alumina and the hydration/dehydration process have been extensively studied by using a variety of techniques,

including vibrational spectroscopies,[5] solid-state NMR spectroscopy,[6] temperature-programmed desorption,[7] calorimetry,[8] as well as theoretical calculations.[4b,9] Despite these efforts, the understanding of surface structures, interactions and properties of γ-alumina is still incomplete, due to the their complex nature.[10]

Solid-state NMR spectroscopy is a versatile tool that can provide both nuclear specific and quantitative local structural information and dynamics of solids at atomic level.[11] It is also well suited for investigating surfaces of oxides where the reactive activities take place, given the short range order present on the surface. Previous studies of γ-alumina based on ^{27}Al or ^{17}O NMR spectroscopy gave little surface structural information, because most of the ^{27}Al ions are in the bulk part of the material which dominate the ^{27}Al NMR spectra. In addition, ^{17}O NMR studies require expensive isotopic enrichment at high temperature prior to the measurement due to the low natural abundance of ^{17}O (0.037 %) and this process is usually not surface-selective, either. Therefore, most of NMR studies focus on ^1H, which uniquely originate from the surface as hydroxyl groups and / or adsorbed water. Consequently, surface-selection can be achieved by correlating other nuclei with surface ^1H species.[12] Surface-selective ^{17}O labelling is also able to assist surface-selection for ^{17}O NMR studies of oxides,[13] however, few results have been reported on alumina.[14] Recently developed dynamic nuclear polarization (DNP) techniques enable NMR studies of surfaces of materials with high sensitivity.[15] For example, ^{27}Al DNP NMR can select the surface of γ-alumina,[6d,16] while ^{17}O 1D/2D NMR studies can be achieved on non-enriched silica samples and ^{17}O 2D/3D NMR investigations can be performed on ^{17}O-enriched silica-alumina with the help of DNP.[17] However, DNP NMR experiments are performed at very low temperatures that may not be compatible with time-resolved spectroscopic investigations of interactions of water and oxides. To the best of our knowledge, real-time/in-situ studies of water interactions on γ-alumina surfaces have not been conducted by NMR spectroscopy, which should provide vital information in the application of the γ-alumina based catalysts, since water is almost always present in catalytic processes.

In this study, solid-state NMR of ^{27}Al, ^1H and ^{17}O, which provides complementary information, was applied to study the interaction of γ-alumina nanorods with water. By adding ^{17}O-enriched water to the sample packed in the NMR rotor and acquiring time-resolved spectra right after the rotor was spun, the surface structure evolution and the interaction with water can be investigated in real-time.

[a] Dr. L. Shen,+ Y. Wang,+ J.-H. Du, Z. Lin, Y. Wen, Prof. L. Peng
Key Laboratory of Mesoscopic Chemistry of Ministry of Education and Collaborative Innovation Center of Chemistry for Life Sciences
School of Chemistry and Chemical Engineering
Nanjing University
Nanjing 210023 (P. R. China)
E-mail: luming@nju.edu.cn
[b] Dr. L. Shen+
Guangling College
Yangzhou University
Yangzhou 225009 (P. R. China)
[c] Dr. K. Chen, Dr. I. Hung, Prof. Z. Gan
National High Magnetic Field Laboratory (NHMFL)
Tallahassee FL-32310 (USA.)
[+] These authors contributed equally to this work.

The XRD pattern of the product of thermally treated boehmite colloidal particles shows that all the diffraction peaks can be indexed to γ-alumina (Figure S1). The irregular rod-like morphology of the sample is revealed by high-resolution transmission electron microscope (HRTEM) image (Figure S2). The surface area and the average pore size of the γ-alumina nanorods are determined as 238 $m^2 \cdot g^{-1}$ and 5.7 nm, respectively (Figure S3).

Similar XRD pattern of γ-alumina nanorods with water added is observed compared to the dehydrated sample (Figure S1), indicating that the interaction of water with γ-alumina can hardly be investigated with XRD. This is not surprising because XRD is a long-range order technique and the surface structure change upon water exposure is only expected to be probed by techniques that are sensitive to local structure, such as solid-state NMR spectroscopy.

^{27}Al MAS NMR spectroscopy was first applied to study the interaction of water with γ-alumina nanorods. The NMR spectrum of dehydrated alumina nanorods obtained at 9.4 T shows two strong peaks with maximum intensity at 63 and 7 ppm, which can be assigned to 4- and 6-coordinated Al ions, respectively (Figure S4a). The resonance due to 6-coordinated Al ions has a much stronger intensity than the 4-coordinated Al, in agreement with the uneven distribution of Al ions between tetrahedral and octahedral sites observed by Lee et al.[18] These two peaks overlap at approx. 25 ppm, thus the presence of 5-coordinated Al ions cannot be excluded.[9c] Time-resolved ^{27}Al MAS NMR data of alumina with water at room temperature shows that the resonant frequencies of the two major peaks owing to 4- and 6-coordinated Al ions remain the same and no additional peak can be observed with the increase of exposure time of water (Figure S4b). The intensities of these peaks vary only slightly with increasing exposure time to water. Furthermore, there is a distribution on the size of ^{27}Al quadrupolar coupling constant (C_Q).[9c] Definitive conclusions can hardly be made at this point due to the relatively poor resolution at a medium external magnetic field.

In order to increase the spectral resolution and distinguish the Al ions with different coordination numbers, ^{27}Al MAS NMR spectra of both dehydrated and hydrated alumina were collected at an ultrahigh field of 35.2 T using the Series-Connected-Hybrid magnet at the National High Magnetic Field Laboratory of the U. S.[19] With the reduction of quadrupole broadening, three peaks at approx. 71, 34 and 12 ppm can be observed for both samples, which can be readily assigned to 4-, 5- and 6-coordinated Al ions, respectively (Figure 1 and Figure S5). The concentration of OH on the surface is expected to be 2–3 OH·nm^{-2} according to the thermal treatment temperature, therefore, 3-coordinated Al species, which have the strongest Lewis acidity, should be completely hydroxylated and cannot be observed here.[2a,9c] The middle frequency peak is very weak compared to the other two peaks, indicating a much lower concentration of 5-coordinated Al ions than 4- and 6-coordinated Al species. Previous reports have shown that the majority of 5-coordinated Al ions are on the surface of γ-alumina while 4- and 6-coordinated Al ions are both in the surface and the bulk part of the material.[3b,6d,14] Since all the Al
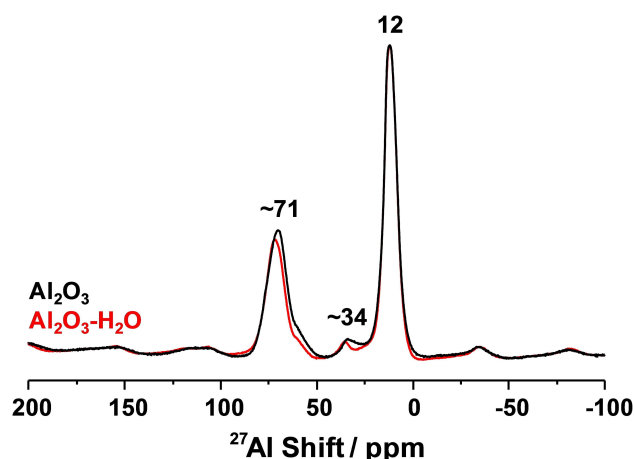
Figure 1. ^{27}Al MAS NMR spectra of dehydrated γ-alumina nanorods and γ-alumina nanorods with H_2O at 35.2 T. Only isotropic peaks are labelled, and all the other peaks are spinning sidebands. Spinning rate: 18 kHz.

species are observed in ^{27}Al MAS NMR (except those associated with extremely large C_Qs thus exceedingly broad linewidths),[9c] and the surface is only a very small fraction of the whole material, even for nanorods with a diameter of around 10 nm in this study (Figure S2), such differences in peak intensities are expected. The relative intensities of Al ions with different coordination numbers vary between the two samples at 35.2 T. The estimated fractions of 4- and 5-coordinated Al ions in hydrated γ-alumina nanorods are smaller than the dehydrated alumina sample (Figure S6 and Table S1).

For NMR of quadrupolar nuclei, the center of gravity of the central transition is shifted from the isotropic chemical shift to a more negative frequency due to second-order quadrupolar interaction, and this shift is the quadrupole induced shift (QIS).[20] Therefore, the larger the C_Q, the larger the QIS and the more negative the observed shift. The calculated C_Qs for 4-coordinated Al species in γ-alumina decrease significantly from 20–28 MHz at 3 OH·nm^{-2} (dehydrated) to 5–10 MHz at 12–15 OH·nm^{-2} (hydrated).[9c] According to these calculations, the QISs should decrease significantly from 17–34 ppm to only 1–4 ppm at 35.2 T.[20] The calculated chemical shifts for 4-coordinated Al sites, on the other hand, are both in the range of 60–80 ppm before and after hydration.[9c] Based on these calculations, the centers of gravity of the peaks owing to 4-coordinated Al should shift to much higher frequencies. For example, some signals arising from 4-coordinated Al species in the dehydrated sample overlap with the signal (~34 ppm) assigned to 5-coordinated Al ions, and these signals should resonate at close to 60–80 ppm in the hydrated sample. Therefore, the effects of hydration on the C_Qs of 4-coordianted Al should cause the peak assigned to 4- and 5-coordinated Al to appear increasing and decreasing in intensity after hydration, respectively. Similar analysis can be performed on 5- and 6-coordinated Al ions. 5-coordinated Al species are associated with medium sized C_Qs which are not very different before (15-18 MHz) and after hydration (13 MHz) based on calculations,[9c] and thus the QISs decrease from 10–14 ppm to 7 ppm.[20] These

decreases of QISs after hydration are much smaller than the case for 4-coordinated Al, thus hydration is expected to cause the peak assigned to 5-and 6-coordinated Al to appear only slightly increasing and decreasing in intensity, respectively. 6-coordinated Al species always have relatively small C_Qs (5-10 MHz) on different water coverages and should be associated with narrow linewidths, therefore, all of 6-coordinated Al species should be observed at 35.2 T before and after hydration.

Therefore, the fraction of 4-coordinated Al species should increase if only the change in C_Qs is effective. The opposite observation suggests that 4-coordinated Al ions are converted to higher coordination Al ions (possibly 5-coordinated Al ions).[4b] Similarly, 5-coordinated Al species are converted to 6-coordinated Al sites, which was also suggested by previous calculation study.[4b] Based on these observations, lower coordinated Al species (4- and 5-coordinated Al) are likely to be converted to Al ions with higher coordination numbers after the adsorption of water (Figure 1). However, the exact fractions of the Al ions on the surface converted can hardly be obtained, because of the large impacts of C_Qs, which have a wide distribution and vary before and after hydration process, on the observed NMR spectral intensity. Again, the differences between the ^{27}Al NMR spectra (Figure 1) are small because the surface Al ions are only a very small fraction of total Al species and surface selective observation can only be achieved by using other structural probes only on the surface, such as ^{1}H and ^{17}O, which have low concentrations in the bulk part of γ-alumina materials.

The surface structure and interactions were then explored with ^{1}H MAS NMR spectroscopy. Three peaks at 2.0, 0.9 and −0.1 ppm arising from different hydroxyl species on the surface of γ-alumina nanorods can be observed in ^{1}H MAS NMR spectrum of the dehydrated sample (Figure 2a). Previous reports show that the chemical shifts are dependent on the number of Al ion connected to the hydroxyl groups.[12,14] The signals (2.0 and 0.9 ppm) with higher frequencies can be assigned to two types of doubly bridging hydroxyl groups (μ^2-OH), while the lower frequency resonance (−0.1 ppm) should arise from an isolated hydroxyl group (μ^1-OH). The triply bridging hydroxyl groups (μ^3-OH) are expected to resonate at around 4.3 ppm,[14] however, the spectral intensity is very small at such frequencies, indicating a very low concentration of this type of hydroxyl species in the dehydrated γ-alumina nanorods.

Time-resolved ^{1}H MAS NMR spectroscopy at room temperature was used to follow the interactions of γ-alumina nanorods with water at different exposure time (Figure 2b). At a minimum exposure time of 4 min, in addition to the peaks owing to hydroxyl species, a sharp and intense signal arising from physisorbed water molecules can be observed at 4.8 ppm. With increasing time, the intensities of the peaks at 2.0, 0.9 and −0.1 ppm increase rapidly, indicating the formation of more μ^2-OH and μ^1-OH species. The formation of hydroxyl species at a very short exposure time (less than several minutes) demonstrates that the surface of γ-alumina nanorods is very reactive with water, which is in agreement with the calculation results on the (110) facets,[4b,21] the predominantly exposed surface on
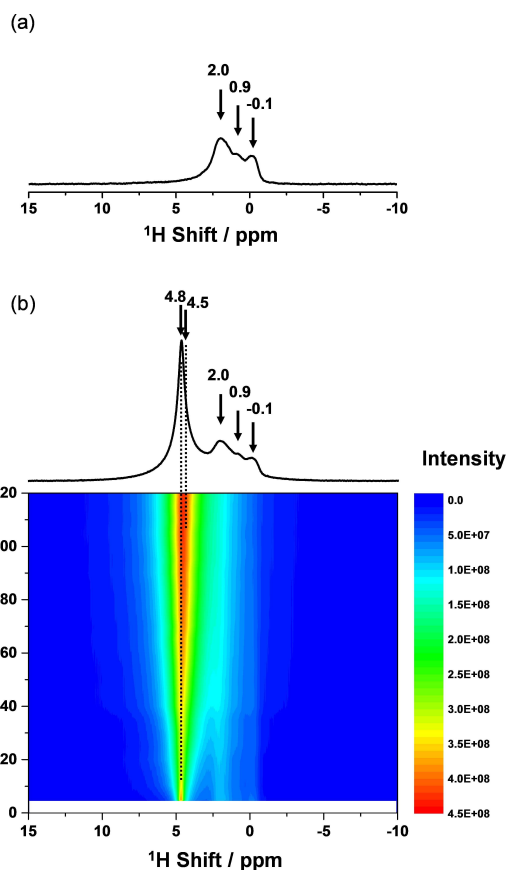
Figure 2. (a) ^{1}H MAS NMR spectrum of dehydrated γ-alumina nanorods. (b) Time-resolved ^{1}H MAS NMR spectra of γ-alumina nanorods with different exposure time to water. The 1D spectrum shown on top corresponds to an exposure time of 10 min. The background signals from the probe and the empty rotor are removed. External magnetic field: 9.4 T; Spinning rate: 14 kHz.
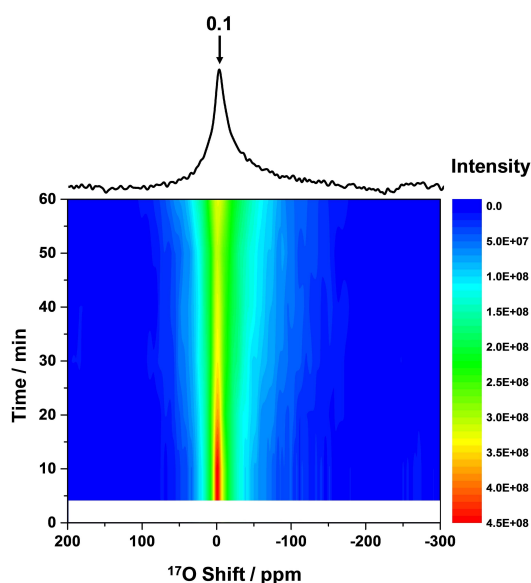
γ-alumina.[22] The intense and sharp peak originated from free water broadens gradually over time and the peak shifts to more negative frequencies. The spectrum does not change much after 2 h, indicating the change on the surface structure upon water exposure mostly occur during this period of time. At this time, the maximum of the major peak is at 4.5 ppm. According to the shift, this resonance centered at 4.5 ppm is assigned to chemisorbed water. It is also possible that some μ^3-OH species form, which resonate at 4.3 ppm,[23] however, no definitive conclusion can be made at this moment. A careful look shows that the spectral intensity of the peak at 4.5 ppm increases with time, presumably due to the relatively short recycle delay used in the experiment and the much shorter longitudinal relaxation time of the chemisorbed water than the physisorbed water. The gradual change of the frequency may also be caused by rapid exchange of protons between water and doubly bridging and isolated hydroxyl groups, as the population of each species varies during the process. Nevertheless, the change in the time-resolved spectral intensities suggests that μ^2-OH and μ^1-OH species are generated.

By using ^{17}O-enriched water, real-time ^{17}O MAS NMR spectroscopy can also be applied to investigate the interaction

of water with γ-alumina at room temperature, even at a medium magnetic field of 9.4 T (Figure 3). Since the [17]O concentration in non-enriched γ-alumina does not allow a spectrum with reasonable signal noise ratio to be obtained at this condition, all the signals come from [17]O-enriched water and its resulting species. The spectra at short exposure times show a sharp resonance at 0 ppm along with a relatively broad component at approx. −25 ppm, which can be tentatively assigned to water and hydroxyl species, respectively. The latter is broad presumably because of a relatively large quadrupolar interaction of hydroxyl sites.[24] The intensity of peak at 0 ppm decreases over time, while the broad resonance centered at around −25 ppm gradually becomes stronger. This change is obvious even in the first 20 minutes, indicating that water can be converted to hydroxyl groups rapidly. It can be understood on the ground that [17]O-water undergoes dissociative adsorption on the low coordinated Al ions on the surface, generating [17]O−H groups, which was previously demonstrated with DFT calculation studies.[4b] It is also in agreement with the time-resolved ^{1}H MAS NMR results and ^{27}Al MAS NMR data at 35.2 T in this study.

^{17}O MAS NMR spectrum was also acquired with a longer water exposure time of 5 h. The data shows the intensity of the relatively sharp resonance at 0 ppm attributed to water is significantly reduced. There is not much change in the broad resonance due to hydroxyl species, judging from the linewidth and spectral intensity, compared to the spectrum of 2 h (Figure S7), which is also consistent with ^{1}H NMR data. However, two relative narrow peaks at 68 and 40 ppm emerge. The high frequencies of these resonances suggest that they should arise from bare oxygen sites in γ-alumina.[24]
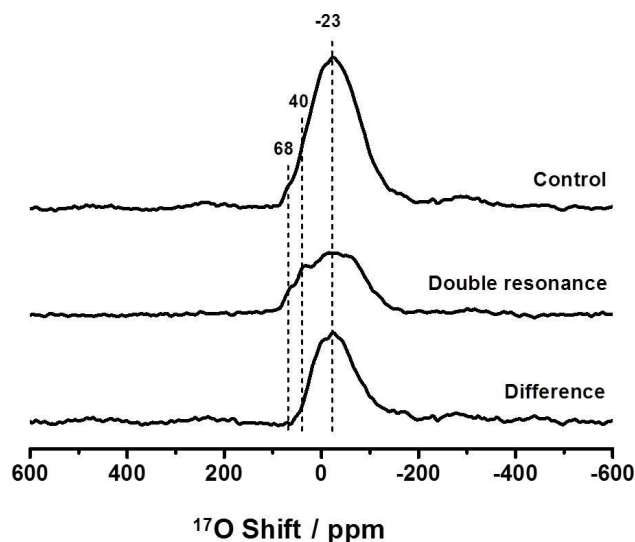
The nature of the resonances observed was further studied with ^{17}O-^{1}H REDOR NMR spectroscopy on the sample 24 h after adding water.[25] The spectrum obtained without dipolar recoupling shows a broad resonance with a maximum at around −23 ppm ("Control" in Figure 4). No sharp component at 0 ppm can be observed, indicating the complete conversion of water to hydroxyl species. Even with a short dipolar recoupling time of only 0.14 ms and a relatively fast spinning speed of 14 kHz, the REDOR NMR spectral intensity of the peak at −23 ppm decreases by about 65 %, confirming this resonance is associated with a very short O−H distance and can be readily assigned to hydroxyl species ("Double resonance" in Figure 4).[11,13a,c,26] The spectrum with dephasing pulses clearly shows two shoulders at 68 and 40 ppm, while these peaks are less obvious in the control experiment and are not observed in the difference spectrum, implying they can be ascribed to oxygen species with a much longer O−H distance than the hydroxyl species. Since no thermal treatment was applied to the sample, the exchange of oxygen ions between the surface and the bulk part of the sample is minimal and all the ^{17}O NMR signal observed should arise from surface oxygen ions. According to the resonant frequencies, these two shoulder resonances at 68 and 40 ppm can now be assigned to bare 4- and 3-coordinated O ions on the surface, which are associated with much smaller quadrupolar interactions.[14] Thus, there is exchange between the oxygen atom in the water molecule and bare surface oxygen ion on γ-alumina. These peaks are not very obvious in the time-resolved ^{17}O MAS NMR spectra in the first hour at 9.4 T (Figure 3), possibly because such exchange process is slow and does not occur with short water exposure time and / or the signal noise ratios at a medium magnetic field is not great.

In order to increase the signal ratios and further investigate this process, time-resolved ^{17}O MAS NMR experiment, as well as ^{17}O MAS NMR experiment of hydrated γ-alumina nanorods were also performed at higher external fields of 19.6 and 35.2 T,

Figure 3. Time-resolved ^{17}O MAS NMR spectra of γ-alumina nanorods with water. The 1D spectrum shown on top corresponds to an exposure time of 10 min. External magnetic field: 9.4 T; Spinning rate: 14 kHz.

Figure 4. ^{17}O-^{1}H REDOR NMR spectra of γ-alumina nanorods with water added (more than 24 h after adding 5 μL water to 100 mg solid). External magnetic field: 9.4 T; spinning rate: 14 kHz; irradiation time in the double resonance experiment: 0.14 ms; v_1(^{1}H): 80 kHz.

respectively. Similar to the data obtained at 9.4 T, a narrow resonance at 0 ppm due to water along with a broad shoulder centered at approx. 18 ppm, which should arise from hydroxyl species, can be observed at 19.6 T (Figure S8). For the hydrated sample, this shoulder arising from hydroxyl is much better resolved at 35.2 T and is centered at approx. 26 ppm (Figure 5). The observation of the hydroxyl groups at −25, 18 and 26 ppm at 9.4, 19.6 and 35.2 T, respectively, is consistent with the estimations based on a quadrupolar coupling constant of about 5.0 MHz.[24] A more closer look at the data in the high frequency region shows that there is a weak but relatively narrow shoulder (compared to the one due to hydroxyl sites) centered at 70.5 ppm even at a very short water exposure time of a few to ten min. (Figure S9). ^{17}O NMR data of hydrated sample obtained at 35.2 T clearly shows a small peak centered at 74 ppm (Figure 5). Only relatively small shifts to higher frequency can be observed from 9.4 (68 ppm) to 19.6 T (70.5 ppm), to 35.2 T (74 ppm), confirming that the peak is associated with a small quadrupolar interaction and it can be assigned to bare 4-coordinated O ions on the surface.[14] Since the lower coordinated sites should be more reactive, the signal due to 3-coordinated O ions is expected at around 40–50 ppm, considering smaller quadrupolar induced shift at a higher external magnetic field.[14] A shoulder at approx. 47 ppm, possibly due to 3-coordinated O ions, can be observed in the spectrum of hydrated γ-alumina at 35.2 T (Figure 5) while such signal is not obvious for the time-resolved spectra at 19.6 T (Figure S8), presumably due to the overlapping with the broad peak attributed hydroxyl species, which is much closer to 40 ppm at higher fields. Nonetheless, the observation of the peak at 68–74 ppm (9.4, 19.6 and 35.2 T) shows that there is fast exchange between the oxygen atom from water and bare surface oxygen ions on γ-alumina nanorods, indicating high reactivity of these sites.
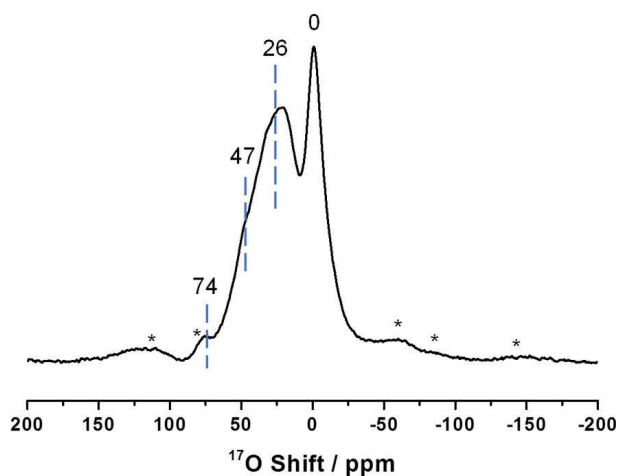
Figure 5. ^{17}O MAS NMR spectrum of γ-alumina nanorods with water. External magnetic field: 35.2 T; Spinning rate: 16 kHz.

In summary, the interaction of γ-alumina nanorods with water was investigated with ^{27}Al, ^{1}H and ^{17}O solid state NMR spectroscopy. To the best of our knowledge, this study is the first report that applies time-resolved MAS NMR spectroscopy and ^{17}O NMR to gain insights into the surface structure change of γ-alumina upon water exposure. Although ^{27}Al MAS NMR spectroscopy is not surface selective, the small differences in the fractions of different ^{27}Al signals in the sample before and after water exposure obtained at an ultrahigh field suggest the involvement of lower coordinated Al in the interaction. Both ^{1}H and ^{17}O NMR spectroscopy provide direct surface structural information. ^{1}H NMR data clearly show formation of μ^2-OH and μ^1-OH hydroxyl species on the surface of γ-alumina nanorods upon exposure to water, which is confirmed with ^{17}O NMR results. ^{17}O NMR data further suggest fast exchange between oxygen atoms in the water molecules and bare surface sites. The data obtained in this study shed light on the dynamics on γ-alumina surface and such methods can be readily extended to investigate the interaction of other oxides with water.

Experimental Section

γ-alumina nanorods were prepared by heating the boehmite colloidal particles (Zhejiang Yuda Chemical Co., Ltd. China) at 823 K for 12 h. The X-ray powder diffraction (XRD) data was obtained on a Shimadzu XRD-6000 diffractometer using Cu Kα radiation ($\lambda =$ 1.5418 Å) operating at 40 kV and 40 mA, with a scan step of 2° in the 2θ range from 20 to 80°. High-resolution transmission electron microscopy (HRTEM) images were collected on a JEOL JEM-2100 instrument with an accelerating voltage of 200 kV. The Brunauer-Emmett-Teller (BET) specific surface area was determined by nitrogen adsorption at −196°C using a Micromeritics Tristar 3020 apparatus. The pore size distribution was derived from the desorption branch of the isotherm by the Barrett-Joyner-Halenda (BJH) method. Solid state NMR experiments at 9.4 T were performed using a Bruker Avance III spectrometer and a 4.0 mm double resonance probe. Solid state NMR data at 19.6 T were recorded with a Bruker Avance NEO spectrometer with a 3.2 mm MAS probe. Solid state NMR spectra at 35.2 T were collected using the series-connected hybrid (SCH) magnet at the NHMFL, a Bruker Avance NEO spectrometer equipped and a costume-made 3.2 mm MAS probe. A single-pulse sequence was used in NMR data acquisition except noted otherwise. The pulse widths for ^{27}Al and ^{17}O NMR are short pulses corresponding $\pi/6$. ^{1}H, ^{27}Al and ^{17}O chemical shifts were externally referenced to adamantane, 0.1 M Al(NO$_3$)$_3$ aqueous solution and H$_2$O at 1.91, 0.0 and 0.0 ppm, respectively. Recycle delays of 1 and 0.1 s are used, for the spectra acquired at 9.4 T and higher fields, respectively. Before the introduction of water, γ-alumina nanorods were heated at 773 K for 12 h under vacuum. For the real-time NMR studies at room temperature, typically, 100 mg nanorod sample was first packed in a MAS rotor and spun at 14 to 20 kHz for a few minutes. After that, the rotor cap was removed and 5 μL common or ^{17}O-enriched water (70%, Cambridge Isotope Laboratories, Inc.) was added in the center of rotor, where an empty space was formed due to fast spinning. This amount of water on the surface corresponds to a fully hydroxylated structure (12.0 OH·nm^{-2} on (110) surface).[27] The rotor was then spun again for NMR data acquisition after the rotor cap was put on tightly. The time between adding water and the start of NMR data acquisition is usually 2 to 4 min. Time-resolved ^{17}O NMR spectra at 9.4 T were collected every 4 min, while all other time-resolved NMR data were recorded every 1 min.

Conflict of Interest

The authors declare no conflict of interest.

[1] B. Youssef, Y. Creff, N. Petit, *Comput. Chem. Eng.* **2012**, *36*, 255–264.

[2] a) R. Wischert, C. Copéret, F. Delbecq, P. Sautet, *Angew. Chem. Int. Ed.* **2011**, *50*, 3202–3205; *Angew. Chem.* **2011**, *123*, 3260–3263; b) L. A. O'Dell, S. L. P. Savin, A. V. Chadwick, M. E. Smith, *Solid State Nucl. Magn. Reson.* **2007**, *31*, 169–173.

[3] a) Q. Yuan, A.-X. Yin, C. Luo, L.-D. Sun, Y.-W. Zhang, W.-T. Duan, H.-C. Liu, C.-H. Yan, *J. Am. Chem. Soc.* **2008**, *130*, 3465–3472; b) J. H. Kwak, J. Hu, D. Mei, C.-W. Yi, D. H. Kim, C. H. F. Peden, L. F. Allard, J. Szanyi, *Science* **2009**, *325*, 1670–1673; c) F. Thibault-Starzyk, E. Seguin, S. Thomas, M. Daturi, H. Arnolds, D. A. King, *Science* **2009**, *324*, 1048–1051; d) Y. Liu, F.-Y. Huang, J.-M. Li, W.-Z. Weng, C.-R. Luo, M.-L. Wang, W.-S. Xia, C.-J. Huang, H.-L. Wan, *J. Catal.* **2008**, *256*, 192–203; e) W. Cai, S. Zhang, J. Lv, J. Chen, J. Yang, Y. Wang, X. Guo, L. Peng, W. Ding, Y. Chen, Y. Lei, Z. Chen, W. Yang, Z. Xie, *ACS Catal.* **2017**, *7*, 4083–4092.

[4] a) M. C. Valero, P. Raybaud, P. Sautet, *J. Phys. Chem. B* **2006**, *110*, 1759–1767; b) M. Digne, P. Sautet, P. Raybaud, P. Euzen, H. Toulhoat, *J. Catal.* **2004**, *226*, 54–68.

[5] a) J. B. Peri, R. B. Hannan, *J. Phys. Chem.* **1960**, *64*, 1526–1530; b) J. B. Peri, *J. Phys. Chem.* **1965**, *69*, 211–219; c) C. C. Chang, *J. Catal.* **1978**, *53*, 374–385; d) C. Dyer, P. J. Hendra, W. Forsling, M. Ranheimer, *Spectrochim. Acta Part A* **1993**, *49*, 691–705; e) A. Boumaza, L. Favaro, J. Lédion, G. Sattonnay, J. B. Brubach, P. Berthet, A. M. Huntz, P. Roy, R. Tétot, *J. Solid State Chem.* **2009**, *182*, 1171–1176.

[6] a) E. C. Decanio, J. C. Edwards, J. W. Bruno, *J. Catal.* **1994**, *148*, 76–83; b) J. J. Fitzgerald, G. Piedra, S. F. Dec, M. Seger, G. E. Maciel, *J. Am. Chem. Soc.* **1997**, *119*, 7832–7842; c) W. Zhang, M. Sun, R. Prins, *J. Phys. Chem. B* **2002**, *106*, 11805–11809; d) D. Lee, N. T. Duong, O. Lafon, G. De Paëpe, J. Phys, *Chem. C* **2014**, *118*, 25065–25076; e) I. B. Moroz, K. Larmier, W.-C. Liao, C. Copéret, *J. Phys. Chem. C* **2018**, *122*, 10871–10882.

[7] a) A. Auroux, R. Monaci, E. Rombi, V. Solinas, A. Sorrentino, E. Santacesaria, *Thermochim. Acta* **2001**, *379*, 227–231; b) M. C. Abello, A. P. Velasco, O. F. Gorriz, J. B. Rivarola, *Appl. Catal. A* **1995**, *129*, 93–100.

[8] a) B. A. Hendriksen, D. R. Pearce, R. Rudham, *J. Catal.* **1972**, *24*, 82–87; b) J. M. McHale, A. Navrotsky, A. J. Perrotta, *J. Phys. Chem. B* **1997**, *101*, 603–613; c) R. H. R. Castro, D. V. Quach, *J. Phys. Chem. C* **2012**, *116*, 24726–24733.

[9] a) M. Digne, P. Sautet, P. Raybaud, P. Euzen, H. Toulhoat, *J. Catal.* **2002**, *211*, 1–5; b) J. Joubert, P. Fleurat-Lessard, F. Delbecq, P. Sautet, *J. Phys. Chem. B* **2006**, *110*, 7392–7395; c) R. Wischert, P. Florian, C. Copéret, D. Massiot, P. Sautet, *J. Phys. Chem. C* **2014**, *118*, 15292–15299.

[10] S. Roy, G. Mpourmpakis, D.-Y. Hong, D. G. Vlachos, A. Bhan, R. J. Gorte, *ACS Catal.* **2012**, *2*, 1846–1853.

[11] J.-H. Du, L. Peng, *Chin. Chem. Lett.* **2018**, *29*, 747–751.

[12] M. Taoufik, K. C. Szeto, N. Merle, I. D. Rosal, L. Maron, J. Trébosc, G. Tricot, R. M. Gauvin, L. Delevoye, *Chem. Eur. J.* **2014**, *20*, 4038–4046.

[13] a) M. Wang, X.-P. Wu, S. Zheng, L. Zhao, L. Li, L. Shen, Y. Gao, N. Xue, X. Guo, W. Huang, Z. Gan, F. Blanc, Z. Yu, X. Ke, W. Ding, X.-Q. Gong, C. P. Grey, L. Peng, *Sci. Adv.* **2015**, *1*, e1400133; b) L. Shen, L. Peng, *Chin. J. Catal.* **2015**, *36*, 1494–1504; c) Y. Li, X.-P. Wu, N. Jiang, M. Lin, L. Shen, H. Sun, Y. Wang, M. Wang, X. Ke, Z. Yu, F. Gao, L. Dong, X. Guo, W. Hou, W. Ding, X.-Q. Gong, C. P. Grey, L. Peng, *Nat. Commun.* **2017**, *8*, 581; d) J. Chen, X.-P. Wu, M. A. Hope, K. Qian, D. M. Halat, T. Liu, Y. Li, L. Shen, X. Ke, Y. Wen, J.-H. Du, P. C. M. M. Magusin, S. Paul, W. Ding, X.-Q. Gong, C. P. Grey, L. Peng, *Nat. Commun.* **2019**, *10*, 5420.

[14] W. Li, Q. Wang, J. Xu, F. Aussenac, G. Qi, X. Zhao, P. Gao, C. Wang, F. Deng, *Phys. Chem. Chem. Phys.* **2018**, *20*, 17218–17225.

[15] A. Lesage, M. Lelli, D. Gajan, M. A. Caporini, V. Vitzthum, P. Miéville, J. Alauzun, A. Roussey, C. Thieuleux, A. Mehdi, G. Bodenhausen, C. Coperet, L. Emsley, *J. Am. Chem. Soc.* **2010**, *132*, 15459–15461.

[16] a) V. Vitzthum, P. Miéville, D. Carnevale, M. A. Caporini, D. Gajan, C. Copéret, M. Lelli, A. Zagdoun, A. J. Rossini, A. Lesage, L. Emsley, G. Bodenhausen, *Chem. Commun.* **2012**, *48*, 1988–1990; b) M. Mais, S. Paul, N. S. Barrow, J. J. Titman, *Johnson Matthey Technol. Rev.* **2018**, *62*, 271–278.

[17] a) F. A. Perras, U. Chaudhary, I. I. Slowing, M. Pruski, *J. Phys. Chem. C* **2016**, *120*, 11535–11544; b) F. A. Perras, Z. Wang, T. Kobayashi, A. Baiker, J. Huang, M. Pruski, *Phys. Chem. Chem. Phys.* **2019**, *21*, 19529–19537.

[18] M.-H. Lee, C.-F. Cheng, V. Heine, J. Klinowski, *Chem. Phys. Lett.* **1997**, *265*, 673–676.

[19] Z. Gan, I. Hung, X. Wang, J. Paulino, G. Wu, I. M. Litvak, P. L. Gor'kov, W. W. Brey, P. Lendi, J. L. Schiano, M. D. Bird, I. R. Dixon, J. Toth, G. S. Boebinger, T. A. Cross, *J. Magn. Reson.* **2017**, *284*, 125–136.

[20] E. Lippmaa, A. Samoson, M. Magi, *J. Am. Chem. Soc.* **1986**, *108*, 1730–1735.

[21] A. Ionescu, A. Allouche, J.-P. Aycard, M. Rajzmann, F. Hutschka, *The J. Phys. Chem. B* **2002**, *106*, 9359–9366.

[22] J.-P. Beaufils, Y. Barbaux, *J. Chim. Phys. Phys.-Chim. Biol.* **1981**, *78*, 347–352.

[23] J. Yang, M. Zhang, F. Deng, Q. Luo, D. Yi, C. Ye, *Chem. Commun.* **2003**, 884–885.

[24] T. H. Walter, E. Oldfield, *J. Phys. Chem.* **1989**, *93*, 6744–6751.

[25] T. Gullion, J. Schaefer, *J. Magn. Reson.* **1989**, *81*, 196–200.

[26] a) L. Peng, Y. Liu, N. Kim, J. E. Readman, C. P. Grey, *Nat. Mater.* **2005**, *4*, 216–219; b) L. Peng, H. Huo, Y. Liu, C. P. Grey, *J. Am. Chem. Soc.* **2007**, *129*, 335–346; c) L. Zhao, Z. Qi, F. Blanc, G. Yu, M. Wang, N. Xue, X. Guo, W. Ding, C. P. Grey, L. Peng, *Adv. Funct. Mater.* **2014**, *24*, 1696–1702; d) L. Shen, X.-P. Wu, Y. Wang, M. Wang, J. Chen, Y. Li, H. Huo, W. Hou, W. Ding, X.-Q. Gong, L. Peng, *J. Phys. Chem. C* **2019**, *123*, 4158–4167.

[27] A. R. Ferreira, E. Küçükbenli, S. de Gironcoli, W. F. Souza, S. S. X. Chiaro, E. Konstantinova, A. A. Leitão, *Chem. Phys.* **2013**, *423*, 62–72.